Magnetic Regulation of Thermo-Chemotherapy from a Cucurbit[7]uril-Crosslinked Hybrid Hydrogel

Haishi Qiao,[†] Jing Jia,[‡] Wei Chen,[†] Bin Di,[‡] Oren A. Scherman,[¶] and Chi Hu[*,†]

†*Department of Pharmaceutical Engineering, China Pharmaceutical University, Nanjing 210009, China*

‡*Key Laboratory of Drug Quality Control and Pharmacovigilance, China Pharmaceutical University, Ministry of Education, Nanjing 210009, PR China*

¶*Melville Laboratory for Polymer Synthesis, Department of Chemistry, University of Cambridge, Cambridge CB2 1EW, United Kingdom*

E-mail: chihu@cpu.edu.cn

List of content

Electrostatic interactions between γ-Fe_2O_3 nanoparticles and CB[7]

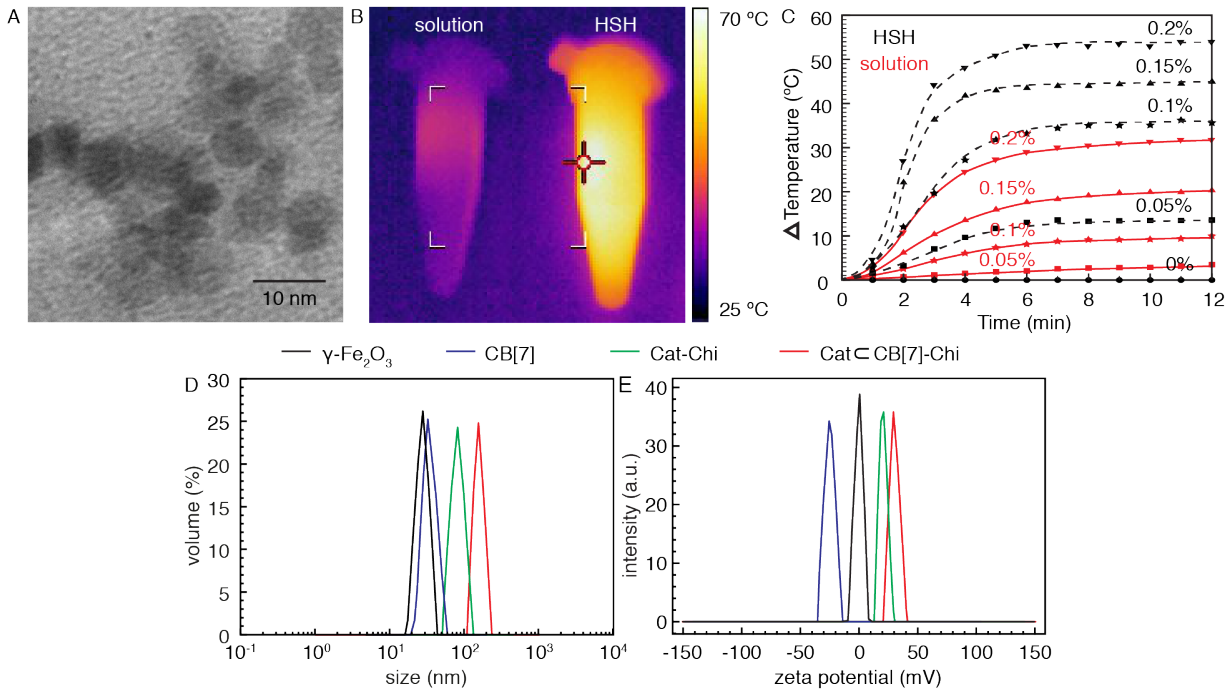

Figure S 1: (A) TEM image of γ-Fe_2O_3 nanoparticles. (B) Infrared thermography images and (C) temperature increase of γ-Fe_2O_3 nanoparticles dissolved in water or encapsulated in HSH. (D) Hydrodynamic diameter and (E) zeta potential of bare and functionalized γ-Fe_2O_3 nanoparticles.

Superparamagnetic γ-Fe_2O_3 nanoparticles with an average diameter of 7 nm were obtained as shown in the TEM image in Figure S1A. γ-Fe_2O_3 nanoparticles (0.1 wt%) dispersed either in water or HSH exhibited different thermal response to applied $\vec{B}$ (5 min) as shown in Figure S1B, where a much more pronounced increase in temperature was observed in HSH. This is likely due to the electrostatic interactions between CB[7] and the γ-Fe_2O_3 nanoparticles, which stabilize the nanoparticles in a well-dispersed form and enhance their magnetic properties. Temperature increase under $\vec{B}$ in either water or HSH while varying the concentration of superparamagnetic nanoparticles is presented in detail in Figure S1C, where unstabilized nanoparticles in water show much less thermal response to the applied magnetic field.

As shown by the solid lines in Figure S1D and E, hydrodynamic diameter D_h and zeta

potential of the prepared bare γ-Fe_2O_3 nanoparticles are 29 nm (PD = 0.09) and -1 mV, respectively. In order to examine the coordination bonding between γ-Fe_2O_3 nanoparticles and the organic components in HSH, γ-Fe_2O_3 nanoparticles (10 mg) were added to an aqueous solution of CB[7] (1 mL, 23 mg, 20 mM), CAT-CS (1 mL, 20 mg, [CAT] = 20 mM) or CAT⊂CB[7]-CS (1 mL, 43 mg, [CAT⊂CB[7]] = 20 mM), and the assembly process was followed by DLS. As shown in Figure S1D, D_h of γ-Fe_2O_3 nanoparticles was increased to 35 nm, 81 nm and 173 nm upon complexation with CB[7], CAT-CS or CAT⊂CB[7]-CS, respectively, inferring the assembly of these organic components on the peripheries of the nanoparticles. γ-Fe_2O_3 nanoparticles show increased D_h upon addition of CAT-CS without CB[7], likely on account of the interactions between CAT motifs and the nanoparticle surface. While having similar molecular structures, CAT⊂CB[7]-CS displays more significant influence on D_h of the nanoparticles compared to CAT-CS, suggesting stronger interactions attributed to the presence of CB[7].

As shown in Figure S1E, zeta potential of γ-Fe_2O_3 nanoparticles was changed to -23 mV, 21 mV and 29 mV upon complexation with CB[7], CAT-CS or CAT⊂CB[7]-CS, respectively. Assembly of CB[7] on the peripheries of the nanoparticles tunes their zeta potential to negative due to the electronegative carbonyl portals of CB[7]. On the contrary, zeta potential of the nanoparticles was changed to positive upon addition of CAT-CS and CAT⊂CB[7]-CS, likely on account of the side-chain amine groups of CS. The positive zeta potential upon addition of CAT⊂CB[7]-CS confirms the formation of coordination bonding between the nanoparticles and CB[7] at the nanoparticles-polymer interface, thus shielding CB[7] and exposing amine groups. Both size measurement and zeta potential analysis conform the electrostatic interactions between γ-Fe_2O_3 nanoparticles and CB[7].

Cell study protocals

HSH was analyzed for cytotoxicity using HeLa cells, which were cultivated in Dulbecco's modified Eagle's medium (DMEM) supplemented with 10 vol% fetal bovine serum and 1 vol%

penicillin and streptomycin (complete growth medium) at 37 °C and 5% CO_2 in a humidified incubator. Cells were grown as monolayer and passaged upon approx. 80% confluence with trypsin (0.25% with EDTA, 3 min). After adding complete growth medium to neutralise the trypsin, cells were harvested from culture medium *via* centrifugation and the supernatant was discarded. Cells were then resuspended in complete growth medium at a concentration of 1.2×10^5 cells per ml in a polystyrene 12-well plate. Cells passages 5-8 were used for cytotoxicity studies.

HSH was cut into discs (12.5 mm diameter, 5 mm height) and placed in complete growth medium at 37 °C for 48 h. HeLa cells were seeded at 1.2×10^5 cells per ml in a polystyrene 12-well plate for 24 h. The cell culture medium was then discarded and replaced by the medium which was used to soak the HSH. The well plate was placed in the incubator for another 24 h. For MTT assay, cells were treated with MTT solution (5 mg/ml) for 4 h at 37 °C. Subsequently, the MTT solution was replaced by DMSO and the absorbance measured at 490 nm. Cell viability was calculated as follows:

$$Cell\ viability = \frac{[A]_{test} - [A]_{medium}}{[A]_{control} - [A]_{medium}} \times 100\% \quad (1)$$

where $[A]_{test}$ is the mean absorbance of test sample, $[A]_{medium}$ is the mean absorbance of culture medium, and $[A]_{control}$ is the mean absorbance of untreated sample.

The HSH exhibits high cell viability (98%) for HeLa cells, indicating potential biocompatibility.

In vivo cargo release

In vivo stability of HSH hydrogels is demonstrated using C57BL/6 mice obtained from Model Animal Research Centre of Nanjing University (Nanjing, China). All animal experiments were carried out in compliance with the Animal Management Rules (Ministry of Health, People's Republic of China) and the Guidance for Care and Use of Laboratory Animals

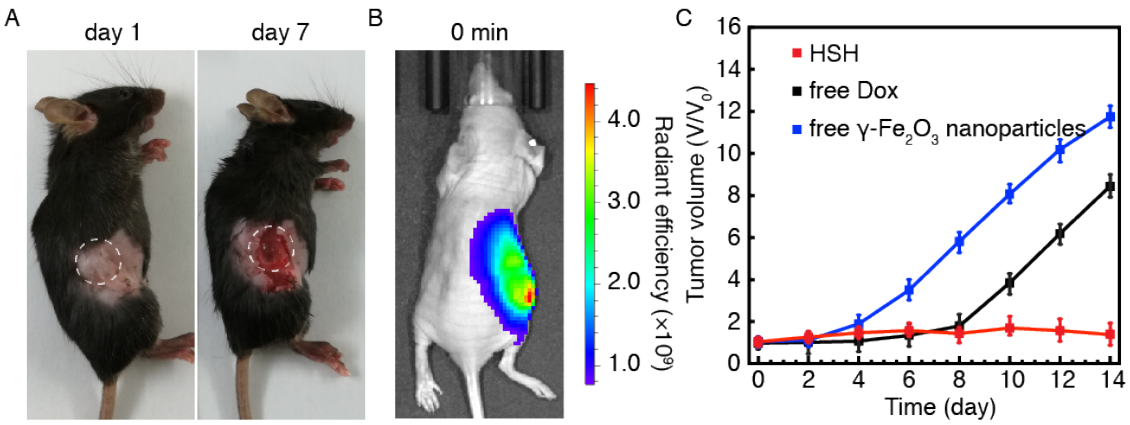

Figure S 2: (A) Representative photographs of HSH hydrogels 7 days after subcutaneous injection in C57BL6 mice showing negligible volume decrease over this time. (B) Intravital fluorescence imaging of mice treated with a buffer solution of ICG. (C) Changes in tumor volume in mice treated with HSH, free Dox or free γ-Fe_2O_3 nanoparticles. Magnetic field was applied for 2 min on day 2, 4, 6, 8, 10 and 12 in all treatment groups.

(China Pharmaceutical University). As shown in Figure S2A, HSH hydrogels reformed immediately following local injection and remained intact for 7 days.

In order to study the *in vivo* cargo release profile, six to eight-week-old athymic nu/nu (BALB/c) mice were 100 µL of ICG-loaded HSH ([ICG] = 100 µM) was injected subcutaneously into the rear right flank of each mouse bearing xenograft tumor (Figure S2B). Treatment groups were injected with ICG-loaded HSH and subjected to $\vec{B}$ for different length of time (0, 2, 4, 6 and 8 min, n=3). Control groups were injected with ICG-loaded HSH and treated in the absence of $\vec{B}$, or injected with a buffer solution of ICG ([ICG]=100 µM, 100 µL, n=2).

Changes in tumor volume in mice treated with HSH, free Dox, or free γ-Fe_2O_3 nanoparticles ([Dox] = 1 mg/mL, [γ-Fe_2O_3] = 0.1 %, 100 µL) are demonstrated in Figure S2C. Only HSH which contains Dox and superparamagnetic nanoparticles in a polymeric matrix through non-covalent interactions shows effective tumor suppression. Pathological inspection of important visceral organs is shown in Figure S3, where no lymphocyte infiltration, necrosis, fibrosis or other abnormal phenomena were observed in the HSH-treated groups.

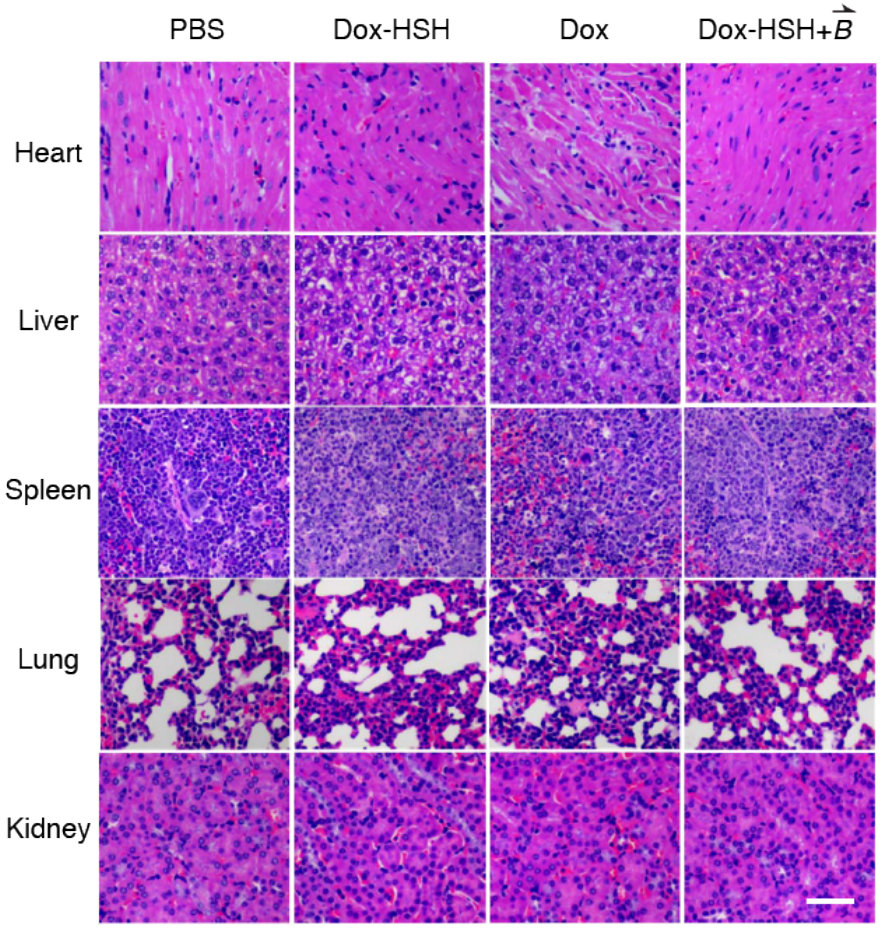

Figure S 3: H&E staining of major organ sections collected from mice treated with PBS buffer, Dox-loaded HSH in the absence of $\vec{B}$, free Dox and Dox-loaded HSH in the presence of $\vec{B}$. Scale bar, 20 μm.